Image Inversion Spectral-Domain Optical Coherence Tomography Optimizes Choroidal Thickness and Detail through Improved Contrast

Phoebe Lin,[1,4] *Priyatham S. Mettu,*[1,4] *Dustin L. Pomerleau,*[1,3] *Stephanie J. Chiu,*[1] *Ramiro Maldonado,*[1] *Sandra Stinnett,*[1] *Cynthia A. Toth,*[1,2] *Sina Farsiu,*[1,2] *and Prithvi Mruthyunjaya*[1]

Purpose. This study was conducted to determine whether there were significant differences in choroidal thickness, contrast, outer choroidal vessel (OCV), and choroidal–scleral junction (CSJ) visualization in inverted versus upright spectral-domain optical coherence tomography (SD-OCT).

Methods. Images were captured on Bioptigen SD-OCT, Zeiss Cirrus HD-OCT, and Heidelberg Spectralis in 42 eyes of 21 healthy subjects. Average choroidal thickness across a fovea-centered 4-mm segment was determined with MATLAB. Quantitative measures of choroidal contrast were measured and CSJ assessed by applying a score of 0 to 3. OCV was determined by counting choroidal vessels $\geq$200 μm.

Results. Mean choroidal thickness was greater in inverted versus upright images captured by Bioptigen ($P \leq 0.003$) and Spectralis ($P \leq 0.015$). Choroidal thickness varied significantly between the three machines ($P < 0.05$). Contrast was higher in inverted versus upright images captured by Bioptigen ($P \leq 0.02$) and Spectralis ($P < 0.001$), but not in Cirrus ($P > 0.10$, both observers). CSJ score was highest in the following: Spectralis inverted = Spectralis EDI > Cirrus upright > Bioptigen inverted. Mean OCV was highest in Spectralis inverted mode.

Conclusion. The most favorable modes to visualize CSJ and OCV are the Spectralis EDI, Spectralis inverted, Cirrus upright, and Bioptigen inverted. These modes demonstrate the highest outer choroidal contrast and choroidal thickness measurements. Choroidal thickness cannot be compared between machines due to conversion factor differences. Future studies and construction of automated segmentation and detection software should take these benefits and pitfalls into account. (*Invest Ophthalmol Vis Sci.* 2012;53:1874–1882) DOI:10.1167/iovs.11-9290

The choroid is composed of three distinct layers: the innermost choriocapillaris, a middle layer of small vessels, and an outer layer of nonfenestrated large caliber vessels adjacent to the sclera.[1,2] In vivo choroidal imaging, by methods such as conventional or high frequency B-scan ultrasonography, A-scan ultrasonography, or partial coherence interferometry,[3,4] has limited ability to resolve the Bruch's inner choroid junction, the choroid–scleral junction (CSJ), and choroidal vascular detail. Even spectral domain-optical coherence tomography (SD-OCT) 820-nm wavelength machines, while excellent at providing retinal detail, are also limited in their ability to resolve choroidal detail for several reasons: (1) poor signal penetration through the retinal pigment epithelium (RPE) and choroid, (2) light beam defocus at the level of the choroid relative to the retina, (3) inadequate contrast between structures of critical interest, and (4) nonideal lateral resolution of the scan.

Placing an OCT device closer to the eye results in an inverted image of the retina and places the outer choroid in closer proximity to the zero-delay line, producing improved choroidal visualization because the choroid represents a lower frequency portion on the Fourier-transformed interferogram compared with standard OCT.[5] Using the Heidelberg Spectralis 820 nm SD-OCT (Heidelberg Engineering, Heidelberg, Germany), Spaide et al.[5] demonstrated that image inversion produced increased depth of field, providing an alternative to using longer wavelength (1040 nm) SD-OCT for better visualization of choroidal detail.[6] In vivo normative data of choroidal thickness according to age was subsequently determined, followed by multiple studies demonstrating changes in choroidal thickness in various ocular diseases.[5,7–10] Duker and colleagues have also examined the ability of the Cirrus HD-OCT (Carl Zeiss Meditec Inc., Dublin, CA) to obtain choroidal thickness in normal subjects.[11]

However, there is currently no well-established metric to objectively assess how clearly the details of the outer choroid are imaged on SD-OCT and no studies have quantitatively validated the subjective perception that inverted imaging

From the [1]Duke Eye Center, Durham, North Carolina; [2]Department of Biomedical Engineering, Duke University, Durham, North Carolina; [3]University of Alabama at Birmingham.

[4]These authors contributed equally to this paper and are co-first authors.

This work was presented in part at the 2011 American Academy of Ophthalmology Annual Meeting, presentation PO516. A portion of this work was also presented at the 2011 Association for Research in Vision and Ophthalmology Annual Meeting, presentations 2858 and 2859.

Supported by the Ronald G. Michels fellowship (PL) and a Heed Foundation fellowship (PSM); a Duke Departmental Research to Prevent Blindness grant (DLP, SF, and PM); and an American Health Assistance Foundation grant (SF). CAT receives research support from both Bioptigen (equipment loan) and Genentech for a study of SD-OCT imaging in age-related macular degeneration. CAT did not participate in image capture or measurements of choroidal thicknesses. Duke University, but not the authors, has a financial interest in Bioptigen.

Submitted for publication December 11, 2011; revised February 16, 2012; accepted February 20, 2012.

Disclosure: **P. Lin**, None; **P.S. Mettu**, None; **D.L. Pomerleau**, None; **S.J. Chiu**, None; **R. Maldonado**, None; **S. Stinnett**, None; **C.A. Toth**, Bioptigen (F), Genetech (F) **S. Farsiu**, None; **P. Mruthyunjaya**, None

Corresponding author: Prithvi Mruthyunjaya, Duke Eye Center, 2351 Erwin Road, Box 3802, Durham, NC 27710.

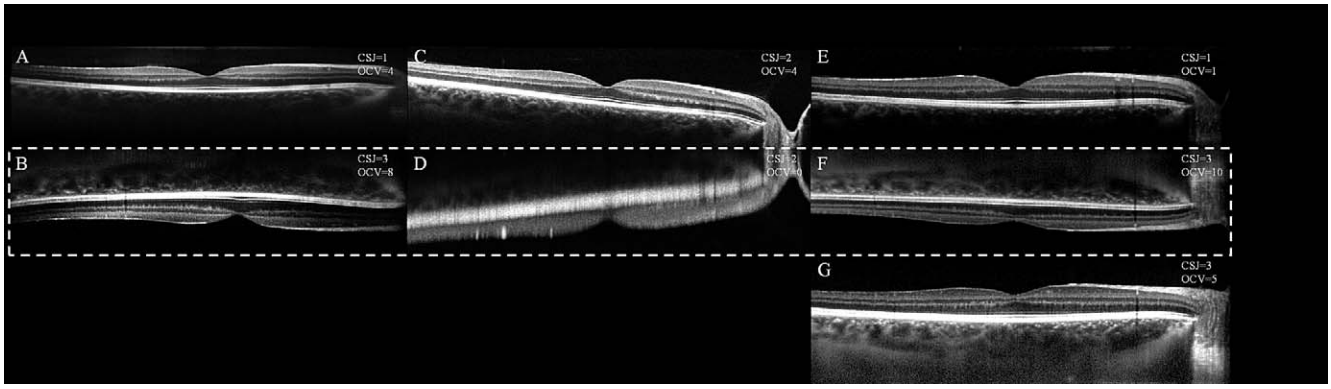

Figure 1. Comparison of upright verses inverted or EDI imaging on Bioptigen (**A, B**), Cirrus (**C, D**), and Spectralis (**E–G**) SD-OCT machines from the same eye. Representative examples of CSJ and OCV scores are given in the upper right corner of each image.

improves visualization of the CSJ and outer choroidal vessels (OCV). Additionally, there are only limited data on how image inversion affects measurements of choroidal thickness among and between various commercially available SD-OCT units.

The goal of this study was three-fold: (1) to determine whether inverted imaging significantly alters choroidal thickness measurements compared with upright images; (2) to define outer choroidal contrast as a metric of choroidal imaging detail and to determine whether image inversion improves outer choroidal contrast; and (3) to determine whether inverted SD-OCT imaging improves subjective visualization of CSJ continuity and large OCV. All aims were assessed across three separate SD-OCT imaging machines.

Methods

Patient Selection and Image Capture Protocol

A prospective, comparative, consecutive case series was performed including 42 eyes of 21 healthy volunteer subjects without known retinal or choroid disease. This research followed the tenets of the Declaration of Helsinki and was approved by the Institutional Review Board. Informed consent was obtained from the subjects after explanation of the nature and possible consequences of the study. Each subject had an ophthalmologic exam including fundoscopy examinations prior to imaging. Exclusion criteria for normal subjects included known or discovered retinal disease (e.g., macular degeneration, drusen, diabetic retinopathy, prior nonsurgical ocular trauma) or glaucoma.

We chose standard SD-OCT imaging parameters currently in clinical use to capture fovea-centered line scans. No research modifications were made to the SD-OCT capture protocols except to use the same settings on all eyes of all patients. For Bioptigen (820 nm, Bioptigen Inc., Research Triangle Park, NC), 9-mm lines scans were captured at the retina. Similarly, for the Heidelberg Spectralis SD-OCT (870 nm), 30° horizontal lines scan yielded approximately 9-mm line scans with small variations between scans. For Bioptigen and Spectralis images, we captured 1536 A-scans per B-scan with 40 averaged B-scans per image. For Cirrus HD-OCT (840 nm), we captured 1024 A-scans per B-scan with 20 averaged B-scans per image using the high-definition (HD) 5-line raster combined into one 9-mm horizontal line scan. There were fewer averaged images on Cirrus because the capture software limited the summed high-resolution scan to a maximum of 20 averaged B-scans, in contrast to the standard number of images obtained on the other two machines.

Manually inverted images were obtained by moving the device closer to the eye to bring the outer choroid into focus at the top of the image, thus placing the zero-delay line closer to the RPE rather than the inner retina (Fig. 1). We obtained one additional image set using the Spectralis enhanced depth imaging (EDI) mode, which is a preset, software-driven algorithm that places the RPE near the zero-delay line while producing an upright enhanced choroidal image without the need to manually push the device closer to the eye (Fig. 1G).

For a given eye, we obtained upright and inverted imaging on three machines and the Spectralis EDI mode, for a total of seven imaging modalities per eye. In both Bioptigen and Spectralis

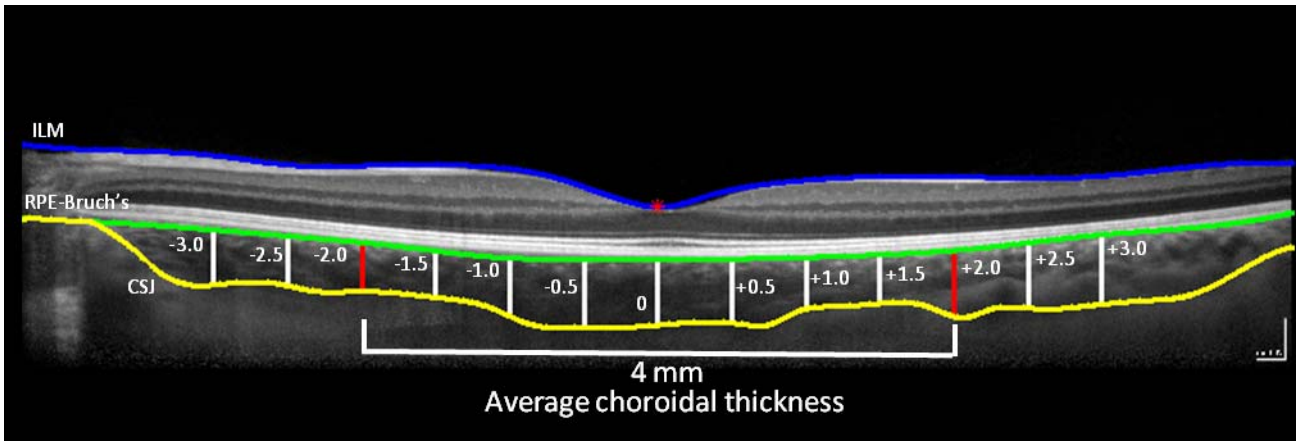

Figure 2. Choroidal and retinal segmentation. Average choroidal thickness and point choroidal thickness measurements are depicted. Red asterisk denotes the foveal center. ILM: internal limiting membrane. RPE, retinal pigment epithelium; CSJ, choroidal-scleral junction.

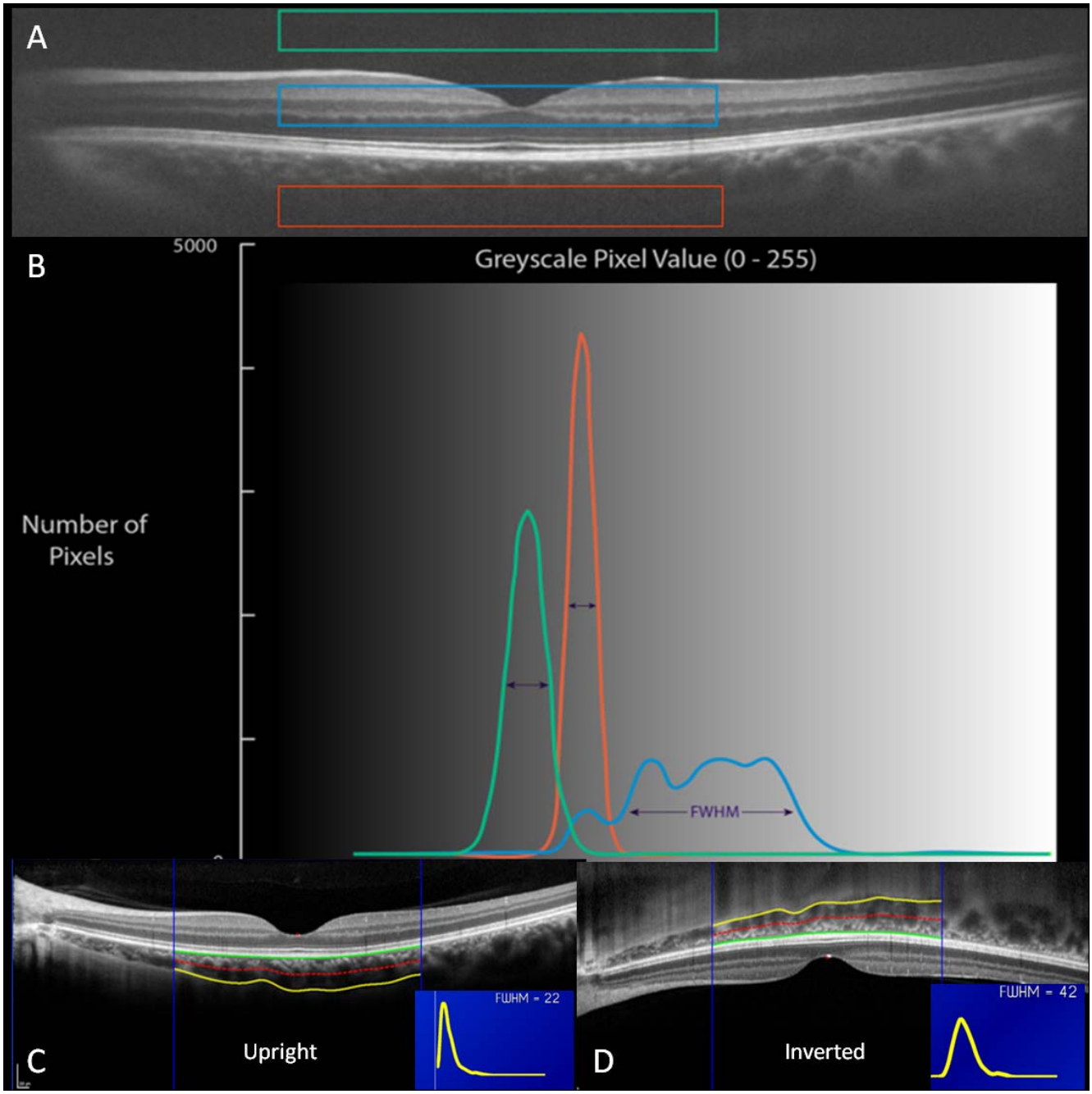

Figure 3. Choroidal contrast (FWHM) measurement method. (**A**) Different areas of OCT image depicted by histograms of grayscale pixel values in (**B**). (**B**) Histograms and FWHM obtained in areas outlined in (**A**). Examples of histograms (insets) and FWHM measurements obtained from the outer choroid (between the dotted red and yellow lines) in (**C**) upright and (**D**) inverted images.

machines, obtaining inverted images did not alter overall detail of the neurosensory retina (Figs. 1A, 1B, 1E–G). In the Cirrus machine, inverting the images resulted in low resolution, highly pixelated images due to a default software mechanism that was put in place to prevent the operator from accidentally obtaining an inverted image (Fig. 1D).[11]

Segmentation, Choroidal, and Retinal Thickness Measurements

We imported all images into a custom program, the Duke OCT Retinal Analysis Program (DOCTRAP), based in MATLAB (Mathworks, Natick, MA), and used DOCTRAP's graphical user interface for manual segmentation. Two experienced masked observers (PL and PSM) each manually segmented the inner and outer borders of the choroid by drawing a line at the inner CSJ and the outer Bruch's line (Fig. 2). The inner retinal surface was segmented by drawing a line at the internal limiting membrane–vitreous junction. We examined a single-point foveal retinal thickness measurement at the center of the fovea, the lowest point on the nerve fiber layer–vitreous boundary, to determine whether inversion creates distortion that could cause differences in observed choroidal thickness.[12]

For choroidal thickness comparisons, average subfoveal choroidal thickness was calculated across a 4-mm choroidal segment centered at

Table 1. Subfoveal Choroidal Thickness Is Higher in Inverted and EDI Compared with Upright Modes, in Bioptigen and Spectralis SD-OCT

Mean Subfoveal Choroidal Thickness (across 4 mm Segment) in Microns (SD)								
	Observer 1			Observer 2			ICC (lower–upper CL)	
$n = 41$	Upright	Inverted	*P* Value	Upright	Inverted	*P* Value	Upright	Inverted
Bioptigen	209.9 (41.9)	228.2 (54.0)	0.003	188.1 (36.8)	214.7 (53.2)	<0.001	0.56 (0.32–0.74)	0.81 (0.67–0.89)
Cirrus	244.3 (56.1)	176.2 (52.5)	<0.001	232.4 (48.6)	242.2 (58.7)	0.237	0.70 (0.50–0.82)	0.16 (0.00–0.45)
Spectralis	223.1 (60.5)	256.2 (65.0)	0.015	227.5 (45.4)	271.1 (80.4)	0.005	0.72 (0.54–0.84)	0.84 (0.72–0.91)
Spectralis EDI	277.1 (86.4)	$P = 0.003$ vs. upright $P = 0.041$ vs. inverted		279.4 (83.2)	$P = 0.002$ vs. upright $P = 0.296$ vs. inverted		0.93 (0.88–0.96)	—

CL, confidence limit; EDI, enhanced depth imaging; ICC, intra-class correlation between Observer 1 and Observer 2; SD, standard deviation.

the fovea (Fig. 2) to circumvent the inherent bias associated with only a single-point choroidal thickness measurement under the central fovea, which can be subject to intra-observer and interobserver variability.[13] We also obtained choroidal thickness point measurements at 500-μm increments nasal and temporal to the foveal reference point (Fig. 2). Axial pixel pitch for the Bioptigen, Cirrus, and Spectralis machines were 3.23, 4, and 3.87 μm/pixel, respectively; these numbers were obtained from the individual SD-OCT companies and were used to convert pixels into thickness measurements in micrometers.

Assessment of Outer Choroidal Contrast

We utilized a quantitative measure of SD-OCT image contrast in the choroidal region based on the full-width at half-maximum (FWHM) of the grayscale pixel value (GPV) histogram. A GPV histogram is a plot of the frequency of occurrence of each GPV, where the horizontal axis represents the grayscale value from 0 to 255 (i.e., dark to bright pixels) and the vertical axis is the number of pixels having this value. The shape of the histogram of a low-contrast region is very similar to the detector noise distribution (often modeled as Gaussian), and its width corresponds to the noise variance (green and red curves in Fig. 3B). Existence of high-contrast anatomical features results in a wider GPV histogram (blue curve in Fig. 3B) and an increased FWHM. For example, choroidal vessel boundaries on SD-OCT appear hyperreflective (large GPV), while the blood appears hyporeflective (small GPV). The higher the contrast of the image, the closer the hyperreflective and hyporeflective GPVs are to 255 and zero, respectively. Thus, the corresponding histogram of an image with high-contrast choroidal vessels is wider than that of a low-contrast image (histograms in Figs. 3C, 3D). We utilize FWHM, which is the width of the histogram at half of its maximum peak, to quantify this phenomenon. As the variability in GPVs increases, the histogram curve becomes wider, and the contrast measure as reflected by FWHM increases. FWHM contrast values can thus be utilized to quantitatively demonstrate the ability of a particular imaging modality to depict heterogeneity in reflectivity and corresponding variability in GPVs.

For each manually segmented image in DOCTRAP as described above, we fitted a spline function to a GPV histogram corresponding to the outer half of the central 4 mm of the choroid. We used MATLAB to calculate and report the FWHM as a measure of relative contrast for the outer choroid in the sub-foveal region (Figs. 3C, 3D).

Assessment of CSJ Continuity and Outer Choroidal Vessel Number

We assessed CSJ continuity across the full 9-mm scan by applying a scoring system in which both observers (PL, PSM) graded the continuity in a masked fashion using the following scale: 0 = no visualization of the CSJ, 1 = <50% CSJ visualized, 2 = 51% to 90% visualized, and 3 = >90% visualized. We assessed visualization of OCV by having each observer (PL, PSM) count the number of large caliber choroidal vessels (≥200 μm) in a masked fashion using a preset 200-μm caliper built into the DOCTRAP segmentation software.

Statistical Analyses

Differences between imaging modes, with respect to choroidal thickness, retinal thickness, choroidal contrast by FWHM, CSJ score, and OCV score, were assessed using generalized estimating equations to account for multiple observations (both eyes). A *P* value of <0.05 was considered statistically significant. Interobserver correlations were determined using intraclass correlations (ICC) according to Bland and Altman.[14]

Results

Demographics

Forty-one eyes of 21 eligible subjects had a full set of seven SD-OCT images. One eye of one subject was excluded because not all protocol images were obtained. All subjects had normal macular fundus examinations. Five subjects were female. The mean age was 32.7 years (range 22–64, SD ±9.1). Sixteen subjects were Caucasian, three were Asian, and two were African-American. Six patients had dark fundus pigmentation, three had light pigmentation, and 12 had moderate pigmentation based on fundus photography and examination. In total, 287 images were segmented and analyzed.

Choroidal Thickness Comparison

Mean subfoveal choroidal thickness values (calculated across a 4-mm choroidal segment centered at the fovea) for each imaging modality are shown in Table 1 for both observers. The mean choroidal thickness was greater (by 18.3 μm, Observer 1; by 26.6 μm Observer 2, $P \leq 0.003$, both observers) for inverted Bioptigen images than for upright Bioptigen images (Figs. 1A, 1B). The difference was also greater (Observer 1: by 33.1 μm; Observer 2: 43.6 μm; $P \leq 0.015$, both observers) for the same comparison on the Spectralis images (Figs. 1E, 1F). Spectralis automated EDI mode (Fig. 1G) had the thickest mean choroidal measurements (Table 1). Inverted imaging on Cirrus had significant variability in choroidal thickness measurements and poor ICC (Table 1) between observers as a result of image pixelation and distortion caused by the default mechanism on image inversion, as described in the methods (Fig. 1D). ICCs of choroidal thickness measurements were highest (≥0.8) in Spectralis EDI > Spectralis inverted > Bioptigen inverted modes.

Differences between upright and inverted (or EDI in Spectralis only) single point choroidal thickness measurements across the entire line scan (at 500-μm increments nasal and temporal to the foveal center) are shown in Figure 4. Maximum

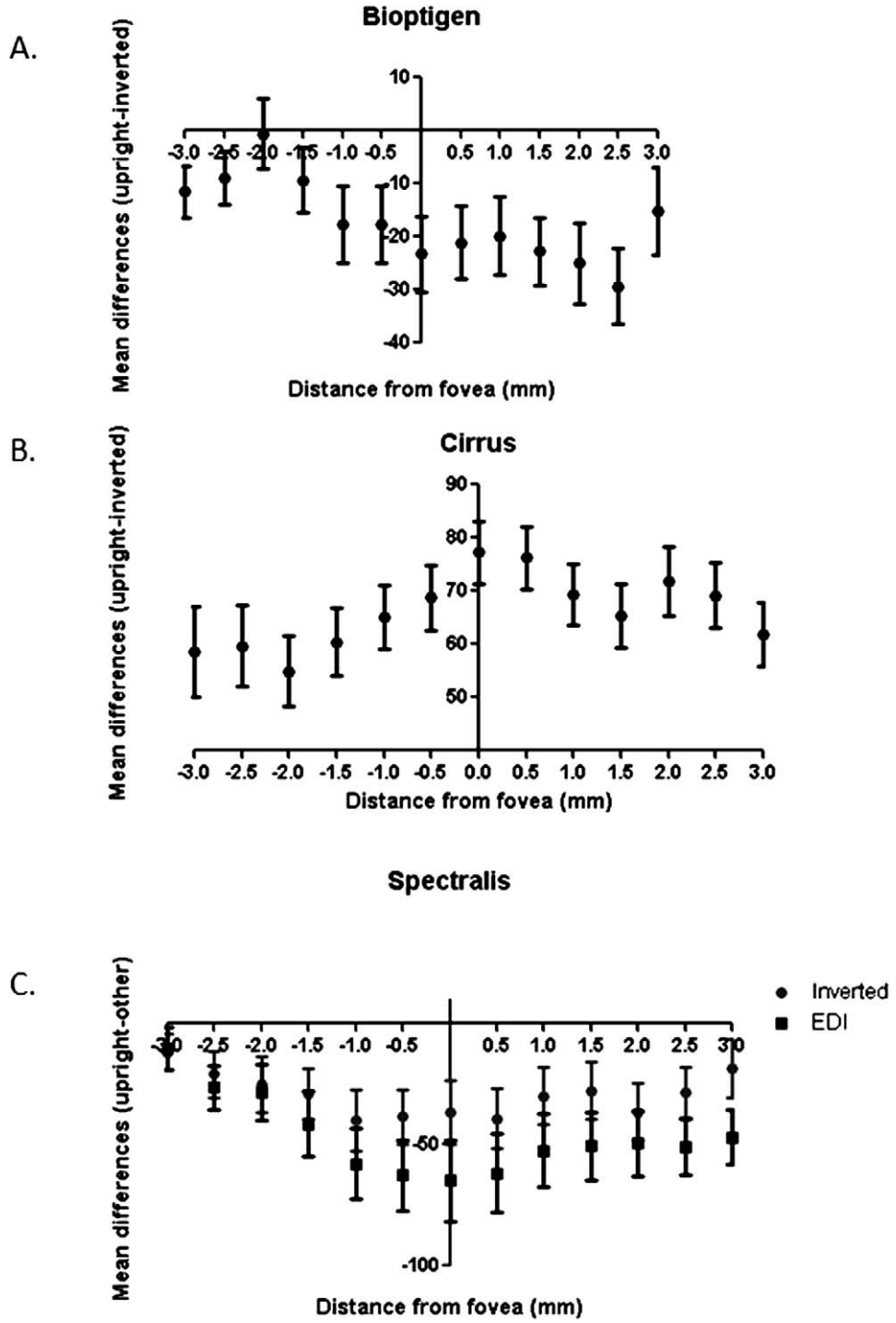

FIGURE 4. Mean of the differences of choroidal thickness at single points relative to the fovea. (**A**) Bioptigen, (**B**) Cirrus, and (**C**) Spectralis. Differences shown represent upright or inverted (or EDI) thicknesses in three SD-OCT machines for Observer 1. Minus sign distances are nasal to the fovea, whereas plus sign distances are temporal to the fovea.

choroidal thicknesses were seen at the fovea, and minimum choroidal thicknesses were found nasal to the fovea in the peripapillary region (not shown). Maximum differences between upright and inverted (or EDI modes) were thus seen at the fovea, and minimum differences in choroidal thickness were generally seen near the nerve (Fig. 4). For Bioptigen and Spectralis machines, inverted images produced higher measured choroidal thickness values compared to upright images at every point. The greatest mean differences were noted with the Spectralis EDI mode (Fig. 4C) compared with the corresponding upright mode. In contrast, inverted Cirrus images produced lower choroidal thickness measurements across the scan than Cirrus upright images as seen by the positive difference values shown in Figure 4B. As evident in Table 1, there was a discrepancy in absolute choroidal thickness measurements between the three machines comparing the same modes ($P < 0.05$), with a larger difference between the Bioptigen and the other two machines, despite

Table 2. Foveal Point Retinal Thickness Measurements Are Similar in Upright and Inverted Modes in Bioptigen and Spectralis and in Upright Mode in Cirrus SD-OCT

	Mean Foveal Point Retinal Thickness in Microns (SD)							
	Observer 1			Observer 2			ICC (lower–upper CL)	
$n = 41$	Upright	Inverted	*P* Value	Upright	Inverted	*P* Value	Upright	Inverted
Bioptigen	209.6 (18.7)	211.4 (20.5)	0.297	207 (21.7)	211.4 (22.4)	0.008	0.91 (0.83–0.96)	0.93 (0.88-0.97)
Cirrus	224.2 (20.0)	318.7 (30.2)	<0.001	221.1 (19.4)	306 (32.4)	<0.001	0.95 (0.91–0.98)	0.79 (0.63-0.90)
Spectralis	230.5 (24.6)	228.6 (26.4)	0.320	226.9 (26.3)	229.2 (25.6)	0.156	0.91 (0.83–0.96)	0.94 (0.88-0.97)
Spectralis EDI	231.8 (28.6)	$P = 0.506$ vs. upright $P = 0.04$ vs. inverted		226 (28.1)	$P = 0.629$ vs. upright $P = 0.04$ vs. inverted		0.94 (0.89–0.97)	—

the images being taken within minutes of each other in the same eyes. This may be a result of how the individual manufacturers developed conversion factors from pixels to micrometer thickness (see Methods), although the method by which these conversion factors were developed was proprietary information and was not revealed to us.

To confirm that choroidal thickness measurements were not influenced by image distortion that may have artifactually increased choroidal thickening, central foveal retinal thickness measurements were compared on the same images. On the Bioptigen and Spectralis machines, there were minimal differences between upright and inverted (or EDI) modes in mean foveal retinal point thickness values for both observers ($\leq$5 μm for all machines) (Table 2). There were large differences between upright and inverted mean foveal retinal thickness values on the Cirrus ($\geq$84.9 μm); the latter difference in retinal thickness is attributable to the distortion encountered in inverted Cirrus images. ICC was higher (all $\geq$0.9) for retinal thickness evaluations than for choroidal thickness evaluations, except in the Cirrus inverted mode. Although central retinal thickness point measurements had high ICC overall, point retinal thickness measurements were again greater overall on Spectralis and Cirrus machines compared with the Bioptigen machine (Table 2). These trends mirrored the apparent differences between machines that were seen in mean choroidal thickness among machines as shown in Table 1.

Outer Choroidal Contrast

Outer choroidal contrast as measured by average FWHM (Table 3) was significantly higher for inverted modes than upright modes in Bioptigen ($P \leq 0.02$, both observers) and Spectralis ($P < 0.001$, both observers) images, but not in Cirrus images ($P > 0.10$, both observers). FWHM was higher in Spectralis EDI images compared with Spectralis upright images ($P < 0.001$, both observers), but not significantly different from Spectralis inverted mode ($P \geq 0.50$, both observers).

Outer Choroidal Detail

CSJ continuity (Table 4) was higher for inverted modes than upright on Bioptigen and Spectralis machines ($P < 0.001$, both observers). CSJ continuity was also higher on Spectralis EDI as compared to upright ($P < 0.001$, both observers). However, Cirrus upright mode scored higher than the inverted mode. CSJ continuity on Cirrus upright images was not significantly different from Bioptigen inverted ($P \geq 0.25$; both observers) images, but was significantly higher than Bioptigen and Spectralis upright modes ($P < 0.001$ for both modes; both observers). The percentage of eyes (out of 41 total) with a score of 2 or higher for CSJ visualization by modality were as follows: Spectralis inverted 100% (both observers) = Spectralis EDI 100% (both observers) > Cirrus upright 100% (Observer 1); 90% (Observer 2) > Bioptigen inverted 97.6% (Observer 1); 90% (Observer 2) > Bioptigen upright 70.7% (Observer 1); 68.3% (Observer 2) > Spectralis upright 68.3% (both observers) > Cirrus inverted 24.4% (Observer 1); 22% (Observer 2). SD-OCT scans with a moderate to excellent visualization of the CSJ (grades 2–3) also had the highest image contrast as measured by FWHM (Fig. 5).

Mean number of OCV visualized was highest with Spectralis inverted and lowest with Cirrus inverted with both observers (Table 5). Cirrus upright images had only a slightly lower mean OCV number than Spectralis inverted mode ($P = 0.04$, Observer 1; $P = 0.065$, Observer 2), but had higher mean OCV number than the upright modes of Bioptigen and Spectralis ($P < 0.001$, both observers). Cirrus upright images scored similarly to Spectralis EDI images ($P \geq 0.2$, both observers). In contrast to choroidal thickness and CSJ continuity where Spectralis inverted and Spectralis EDI were similar, Spectralis inverted images had a higher mean OCV count than Spectralis EDI mode ($P \leq 0.001$, both observers).

Table 3. Outer Choroidal Image Contrast Values Are Higher in Inverted (and EDI) Modes Compared With Upright Modes in Bioptigen and Spectralis

	Mean FWHM in Grayscale Pixel Values (SD)							
	Observer 1			Observer 2			ICC (lower–upper CL)	
$n = 41$	Upright	Inverted	*P* Value	Upright	Inverted	*P* Value	Upright	Inverted
Bioptigen	20.6 (5.2)	23.1 (8.4)	0.017	21.1 (5.2)	24 (8.8)	0.009	0.82 (0.69–0.90)	0.93 (0.87–0.96)
Cirrus	27.9 (10.1)	29.5 (9.5)	0.196	28.2 (9.5)	27.4 (8.7)	0.579	0.95 (0.90–0.97)	0.77 (0.61–0.87)
Spectralis	29.9 (13.6)	39.1 (12.7)	<0.001	28.1 (12.1)	38.7 (11.8)	<0.001	0.92 (0.85–0.95)	0.87 (0.76–0.93)
Spectralis EDI	38.5 (12.5)	$P < 0.001$ vs. upright $P = 0.748$ vs. inverted		37.4 (11)	$P < 0.001$ vs. upright $P = 0.506$ vs. inverted		0.85 (0.73–0.91)	—

Table 4. Choroid-Scleral Junction Visualization Is Higher in Inverted (and EDI) Compared with Upright Modes in Bioptigen and Spectralis

	Mean CSJ Score (SD)							
	Observer 1			Observer 2			ICC (lower–upper CL)	
$n = 41$	Upright	Inverted	*P* Value	Upright	Inverted	*P* Value	Upright	Inverted
Bioptigen	2.0 (0.8)	2.6 (0.5)	<0.001	2.0 (0.8)	2.4 (0.7)	<0.001	0.98 (0.96–0.99)	0.74 (0.57–0.85)
Cirrus	2.7 (0.5)	1 (0.8)	<0.001	2.5 (0.7)	0.9 (0.8)	<0.001	0.79 (0.64–0.88)	0.85 (0.73–0.91)
Spectralis	2.0 (0.8)	2.9 (0.3)	<0.001	2.0 (0.8)	2.9 (0.3)	<0.001	0.97 (0.94–0.98)	1.0
Spectralis EDI	3.0 (0.2)	$P < 0.001$ vs. upright $P = 0.060$ vs. inverted		2.9 (0.3)	$P < 0.001$ vs. upright $P = 0.136$ vs. inverted		0.79 (0.64–0.88)	—

Grading scale for CSJ continuity: 0 = no visualization of the CSJ, 1 = <50% CSJ visualized, 2 = 51% to 90% visualized, and 3 = >90% visualized.

Discussion

To our knowledge, this is the first prospective comparison of choroidal thickness and contrast measurements in inverted versus upright imaging across multiple SD-OCT systems. We found that Spectralis and Bioptigen inverted images (or Spectralis EDI mode) yielded significantly higher choroidal thickness and contrast measurements than upright modes. The significant increase in measured choroidal thickness in inverted images compared with upright images was likely due to improved choroidal contrast and better visualization of the CSJ. In other words, when contrast is poor in the outer choroid and the CSJ is not well-visualized due to poor OCT penetration, manual segmentation of the CSJ occurs closer to the RPE-Bruch's junction where the choroidal reflectivity drops to background levels, thus resulting in thinner choroid measurements. Upright Cirrus images had significantly higher CSJ and OCV values than the upright modalities of the other two machines, suggesting that the Zeiss Cirrus proprietary image capture software may set the zero delay line in a location that equally favors imaging of the retina and choroid, while the Bioptigen and Spectralis software may favor clarity of the retinal image in the upright mode.

Mean choroidal thickness measurements were lower than previously published reports[5,11,13] because our technique measured average choroidal thickness over a 4-mm segment, rather than at a single point under the central fovea (the thickest part of the choroid), to avoid any intra- and interobserver variability associated with subjective placement of calipers at a single point for measurements.[13] For comparison, we separately obtained single-point choroidal thickness measurements by interpolation using MATLAB software. The latter values were more consistent with previously published reports (data not shown),[5,11,13] but remained slightly lower, possibly due to differences in patient population and measurement methodology. Future reports of subfoveal choroidal thickness should consider utilizing our averaging method.

We observed a discrepancy in absolute choroidal thickness measurements between the three machines. Diurnal shifts in choroidal blood flow resulting in changes in choroidal

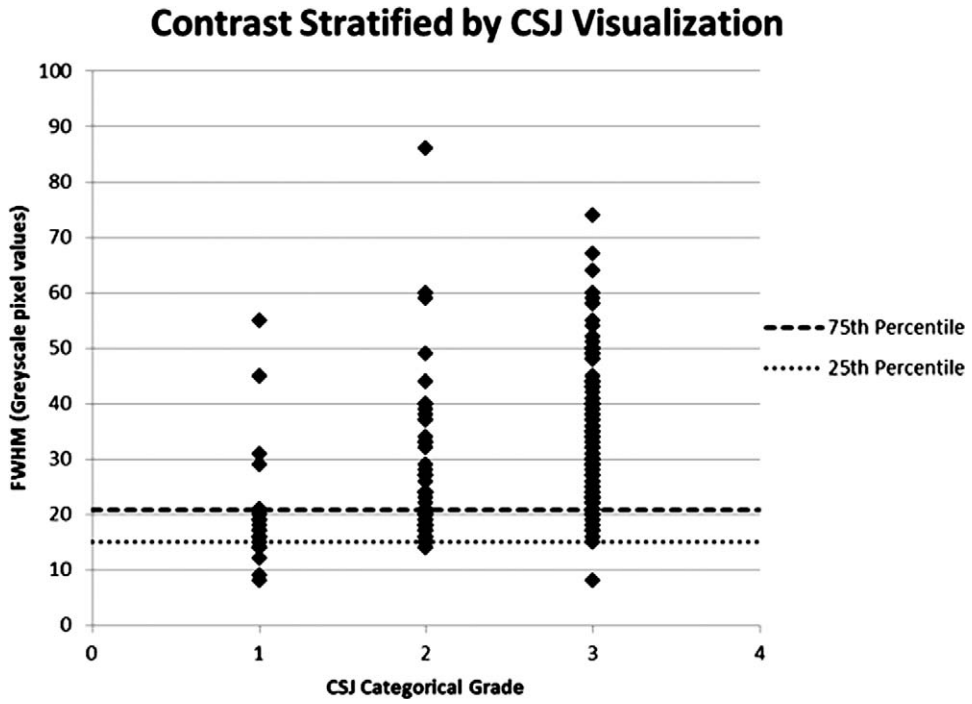

Figure 5. Outer choroidal contrast, as measured by full width at half maximum (FWHM) in GPVs, was plotted for all images (except Cirrus inverted, which contained significant artifact), according to categorical grade of CSJ continuity: 0 = no visualization of the CSJ; 1 = <50% CSJ visualized; 2 = 51% to 90% visualized, and 3 = >90% visualized. Dashed line represents 75th percentile of the distribution of contrast values in grade 1, while the dotted line represents the 25th percentile of the same distribution.

Table 5. Visualization of Outer Choroidal Vessels Is Higher in Inverted (and EDI) Compared with Upright for Bioptigen and Spectralis

	Mean Number of OCV (SD)							
	Observer 1			Observer 2			ICC (lower–upper CL)	
$n = 41$	Upright	Inverted	*P* Value	Upright	Inverted	*P* Value	Upright	Inverted
Bioptigen	2.4 (1.9)	5.5 (2.7)	<0.001	2.7 (1.8)	6.1 (2.7)	<0.001	0.83 (0.71–0.91)	0.86 (0.75–0.92)
Cirrus	7.0 (2.9)	0.5 (0.7)	<0.001	6.5 (2.5)	0.6 (0.9)	<0.001	0.85 (0.74–0.92)	0.77 (0.60–0.87)
Spectralis	3.2 (3.0)	8.0 (2.9)	<0.001	3.9 (2.7)	7.5 (3)	<0.001	0.84 (0.73–0.91)	0.89 (0.80–0.94)
Spectralis EDI	6.2 (2.9)	$P < 0.001$ vs. upright $P < 0.001$ vs. inverted		6.4 (2.7)	$P < 0.001$ vs. upright $P = 0.001$ vs. inverted		0.87 (0.76–0.93)	—

thickness is an unlikely cause[15] since the images were obtained within a few minutes of each other. A second explanation may be the potential inaccuracy of factors used to determine the axial pixel pitch ratio for converting pixel measurements to actual tissue thickness even though these values were corroborated with technical experts at the corresponding SD-OCT companies based on manufacturer-specific methods. To eliminate the potential confounder that our segmentation software introduced error into these measurements, we compared subfoveal point choroidal thickness measurements obtained using our segmentation software to those obtained using the proprietary software of each machine and found that there was no difference (data not shown). The trends among different machines in terms of a completely different measure, the foveal point retinal thickness, mirror the differences between machines in choroidal thickness, with Bioptigen measurements significantly thinner than either Cirrus or Spectralis images. This again may be due to proprietary configurations in axial pixel pitch ratios provided by the manufacturers.

The above factors limit our ability to directly compare choroidal thickness measurements reliably between machines or comment on their ability to approximate true choroidal thickness in the absence of a gold standard. Histological sections from cadaveric eyes do not reveal true in vivo thickness of the choroid due to fixation artifacts.[16] Other methods of in vivo choroidal imaging such as partial coherence interferometry have resulted in a mean choroidal thickness measurement of 293.4 μm for patients in an age range similar to our study.[3] This number correlates well with measurements taken in Spectralis EDI mode but is quite disparate from Bioptigen measurements in the current study.

Pixelated, low-resolution scans were obtained with inversion on Cirrus, due to the machine's software default. This resulted in considerable variability in choroidal thickness measurements and low ICC between observers, which were due in part to image distortion on inverted Cirrus scans, as evidenced by the large difference in retinal thickness measurements between upright and inverted Cirrus modes. While differences in upright and inverted retinal thicknesses were found to have statistical significance in Bioptigen for Observer 2, these differences were all less than 5 μm which is unlikely to be clinically significant. In other words, increased choroidal thickness with image inversion on Bioptigen and Spectralis (and for Spectralis EDI) was not likely to be attributable to image distortion, whereas image distortion was likely a factor in the measured decrease in choroidal thickness seen with inversion in Cirrus. Bioptigen and Spectralis inverted imaging (as well as EDI mode) provided higher outer choroidal contrast than upright imaging. This was not true in Cirrus, for which inverted imaging created artificially high contrast. Additionally, ICC was high for all inverted modes other than Cirrus.

We found that SD-OCT scans with moderate to excellent visualization of the CSJ (grades 2–3) had much higher contrast measurements than eyes with poor CSJ visualization (grade 1). Thus, the proposed criterion of contrast appears to be a quantifiable and reproducible measure of outer choroidal detail on SD-OCT images. While there was variance in FWHM values within each grade of CSJ visibility, this was probably due to the fact that outer choroidal contrast was measured only in the central 4 mm, and CSJ continuity was assessed for the entire foveal image.

Ikuno et al.[17] compared choroidal thickness measurements between EDI images captured on a Heidelberg Spectralis machine to a long-wavelength or high penetration OCT machine (HP-OCT, 1060 nm). They found that choroidal thicknesses correlated well between the two machines suggesting that there may be little need for a high penetration machine if the purpose is to simply measure choroidal thickness. The investigators did not address visualization of choroidal detail as we have done in our study. Future studies comparing outer choroidal contrast and visualization of outer choroidal detail between inverted (or EDI) SD-OCT and HP-OCT machines would be warranted to address this issue.

Although we do not think that reliable thickness comparisons can be made between the three different machines, we did compare their ability to visualize the CSJ and OCV, since this does not implement any inherent conversion factor differences. Cirrus upright, Spectralis inverted, and Spectralis EDI yielded the highest CSJ scores, although Bioptigen inverted images scored nearly as high for CSJ. Lower choroidal thickness measurements were obtained in the presence of low CSJ scores (within a machine). This is most likely because in the absence of a well-defined CSJ, the observer tends to segment the inner CSJ closer to the RPE-Bruch's line, where the choroidal signal changes to a background level of signal in the upright mode as mentioned above. However, it is important to note that like choroidal thickness measurements, there is no gold standard for determining the precise location of the CSJ. Another factor confounding the true versus imaged location of the CSJ may be the histological designation of the lamina fusca, the innermost portion of the sclera that transitions into the choroid. The lamina fusca will sometimes contain choroidal vessels between scleral fibrils making it difficult to establish a continuous CSJ and to define OCV with precision.

Contrast (FWHM), CSJ continuity, and OCV visualization are parameters that, unlike choroidal thickness, do not rely on conversion factors specific to the machine, which allows comparison across different machines. The average number of OCV visualized was highest in Spectralis inverted images but only minimally differed from the Spectralis EDI and Cirrus upright modes. We recognize, however, that there are limitations to this comparison, such as the inability to guarantee that precisely the same cross-section of the choroidal vasculature is obtained with each machine.

The primary strength of our study as compared to other previously published studies on inverted SD-OCT is its prospective design, which minimizes possible selection bias for images with excellent CSJ visualization or choroidal vessel detail. One limitation of our study is that it included younger subjects without macular pathology, which limits its generalizability to older individuals, in which visualization of the outer choroid might be enhanced due to age-related choroidal atrophy.[18] Also, it is difficult to determine whether similar results would be obtained in patients with macular pathology.

In summary, the most favorable modes to visualize CSJ, OCV, and measure choroidal thickness are the Spectralis EDI, Spectralis inverted, Cirrus upright, and Bioptigen inverted modes due to optimized contrast. Comparisons of choroidal thickness among machines are not possible given the differences in machine-specific conversion factors. However, comparisons of choroidal thickness can be made within the same machine using the same mode. To the best of our knowledge, our study is the first to demonstrate that inverted SD-OCT imaging optimizes visualization of CSJ and choroidal vessels through improved outer choroidal contrast. We have established contrast as a valid quantifiable measure of choroidal image quality and explored the optimal imaging modalities for choroidal vessel detail and choroidal thickness measurements. These findings will serve as a necessary foundation for the development of reliable, automated choroidal segmentation software, and for the creation of a semi-automated algorithm for assessing patterns of outer choroidal vasculature in physiologic and pathologic states. Future studies using inversion choroidal imaging or EDI should be cautioned against directly comparing choroidal thickness measurements between different machines.

References

1. Hayreh SS. Vascular pattern of the choriocapillaris. *Exp Eye Res*. 1974;19:101–104.
2. Hayreh SS. Segmental nature of the choroidal vasculature. *Br J Ophthalmol*. 1975;59:631–648.
3. Brown JS, Flitcroft DI, Ying GS, et al. In vivo human choroidal thickness measurements: evidence for diurnal fluctuations. *Invest Ophthalmol Vis Sci*. 2009;50:5–12.
4. Coleman DJ, Silverman RH, Chabi A, et al. High-resolution ultrasonic imaging of the posterior segment. *Ophthalmology*. 2004;111:1344–1351.
5. Spaide RF, Koizumi H, Pozzoni MC. Enhanced depth imaging spectral-domain optical coherence tomography. *Am J Ophthalmol*. 2008;146:496–500.
6. Jaillon F, Makita S, Min EJ, Lee BH, Yasuno Y. Enhanced imaging of choroidal vasculature by high-penetration and dual-velocity optical coherence angiography. *Biomed Opt Express*. 2011;2:1147–1158.
7. Fong AH, Li KK, Wong D. Choroidal evaluation using enhanced depth imaging spectral-domain optical coherence tomography in Vogt-Koyanagi-Harada disease. *Retina*. 2011;31:502–509.
8. Fujiwara T, Imamura Y, Margolis R, Slakter JS, Spaide RF. Enhanced depth imaging optical coherence tomography of the choroid in highly myopic eyes. *Am J Ophthalmol*. 2009;148:445–450.
9. Maruko I, Iida T, Sugano Y, et al. Subfoveal choroidal thickness after treatment of Vogt-Koyanagi-Harada disease. *Retina*. 2011;31:510–517.
10. Spaide RF. Enhanced depth imaging optical coherence tomography of retinal pigment epithelial detachment in age-related macular degeneration. *Am J Ophthalmol*. 2009;147:644–652.
11. Manjunath V, Taha M, Fujimoto JG, Duker JS. Choroidal thickness in normal eyes measured using Cirrus HD optical coherence tomography. *Am J Ophthalmol*. 2010;150:325–329. e321.
12. Chiu SJ, Li XT, Nicholas P, Toth CA, Izatt JA, Farsiu S. Automatic segmentation of seven retinal layers in SDOCT images congruent with expert manual segmentation. *Opt Express*. 2010;18:19413–19428.
13. Rahman W, Chen FK, Yeoh J, Patel P, Tufail A, Da Cruz L. Repeatability of manual subfoveal choroidal thickness measurements in healthy subjects using the technique of enhanced depth imaging optical coherence tomography. *Invest Ophthalmol Vis Sci*. 2011;52:2267–2271.
14. Bland JM, Altman DG. Statistical methods for assessing agreement between two methods of clinical measurement. *Lancet*. 1986;1:307–310.
15. Chakraborty R, Read SA, Collins MJ. Diurnal variations in axial length, choroidal thickness, intraocular pressure, and ocular biometrics. *Invest Ophthalmol Vis Sci*. 2011;52:5121–5129.
16. Brown NH, Koreishi AF, McCall M, Izatt JA, Rickman CB, Toth CA. Developing SDOCT to assess donor human eyes prior to tissue sectioning for research. *Graefes Arch Clin Exp Ophthalmol*. 2009;247:1069–1080.
17. Ikuno Y, Maruko I, Yasuno Y, et al. Reproducibility of Retinal and Choroidal Thickness Measurements in Enhanced Depth Imaging and High-Penetration Optical Coherence Tomography. *Invest Ophthalmol Vis Sci*. 2011;52:5536–5540.
18. Spaide RF. Age-related choroidal atrophy. *Am J Ophthalmol*. 2009;147:801–810.